Modeling and Control of a Radio-Controlled Model Racing Car

T.C.J. Romijn **W.H.A. Hendrix** **M.C.F. Donkers**

Dept. Electical Eng., Eindhoven University of Technology, Netherlands
(e-mail: t.c.j.romijn@tue.nl, w.h.a.hendrix@tue.nl, m.c.f.donkers@tue.nl)

Abstract: This paper presents an experimental platform and a modeling and control challenge posed to second-year Bachelor students in Automotive Engineering at Eindhoven University of Technology. The experimental platform consists of a customized radio-controlled 1:5-scale model racing car. The car consists of a digital signal processor, which can be programmed using Simulink, two motors, each driving one rear wheel, and sensors to measure the wheel speeds and the jaw rate. The radio-controlled car is used to give students hands-on experience in modeling and control, which is essential for a well-balanced control education. In this paper, it is shown that the radio-controlled car can be modeled using a bicycle model, which shows that this simple model can capture the essential vehicle dynamics. Furthermore, both a solution for torque vectoring and traction control are presented and demonstrated in this paper using the developed experimental platform.

Keywords: Demonstrator, Control Education, Vehicle Dynamics, Traction Control

1. INTRODUCTION

Hands-on experience is an essential part of a well-balanced educational program for students. Industry requires students to not only have theoretical knowledge, but also the ability to apply it in practice. Developing experimental platforms that give students hands-on experience is challenging. The experimental platforms should be motivating and pose a good (control-oriented) engineering problem that is relevant for today's industry. Moreover, experimental setups should teach students about designing experiments and dealing with practical limitations induced by, e.g., low grade sensors.

To offer students this practical experience and to train them in developing their practical skills, a radio-controlled (RC) model racing car has been developed. This RC model racing car has two electric motors, each driving one rear wheel, and sensors for measuring the throttle input, the steering input, the individual wheels speeds and the yaw rate of the vehicle. Because of the two electric motors, the torque to each of the rear wheels can be controlled separately. The concept of torque vectoring exists in many varieties, e.g., an overview for feedback control techniques for torque-vectoring control of fully electric vehicles is given in (De Novellis et al., 2014). The combination of active front steering with rear torque vectoring actuators is used in an integrated controller to guarantee vehicle stability/trajectory tracking is discussed in (Bianchi et al., 2010) and torque vectoring with a feedback and feed forward controller is proposed in (Kaiser et al., 2011). Another application of torque vectoring is by braking individual wheels in order to stabilize the vehicle which is generally available in today's cars on the road, e.g., electronic stability controllers are presented in (Rajamani, 2006; Piyabongkarn et al., 2007). This demonstrates the relevance of the topic in today's automotive industry.

The control challenge posed to second-year Bachelor students is to improve the handling of the RC racing car by designing and implementing torque control for each of the rear wheels. To do this, a good theoretical knowledge of vehicle dynamics is necessary, e.g., the concepts of understeer/oversteer and dynamic weight transfer (Pacejka, 2005). This knowledge is used to design a simulation model that has to be tuned and verified/validated using experimental data. This is challenging as students need to find the right balance between model complexity and accuracy. The model can then be used to design a controller and to analyze its closed-loop behavior in a simulation environment. Finally, the controller is implemented on a digital signal processor (DSP) that is mounted on the RC car and can be programmed using Matlab/Simulink.

This paper describes the RC model racing car and explains the modeling and control challenges. In particular, the hardware and software of the experimental setup will be explained in Section 2. In Section 3, we will show

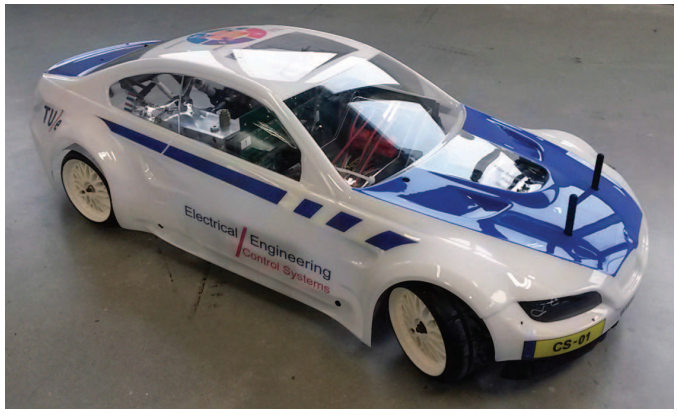

Fig. 1. The radio-controlled model racing car

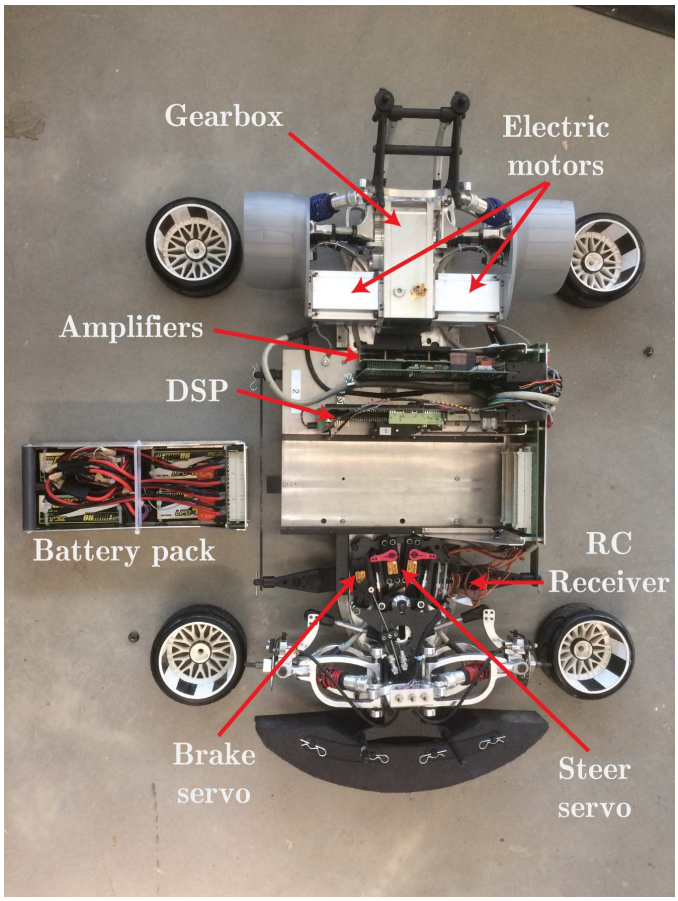

Fig. 2. Hardware layout of the RC model racing car

that a single-track bicycle model can be used to describe the cornering behavior of the car. In Section 4, we will show a typical control solution that students can come up with, which is implementable and improves the vehicle handling. Section 5 is used to demonstrate the proposed control solutions on the experimental setup. Finally, some concluding remarks will be made in Section 6.

2. EXPERIMENTAL SETUP

In this section, the RC model car hardware and software platform is described. The chassis of the RC racing car is a FG Competition EVO 08-510 shown in Figure 1. The scale of the model is 1:5, i.e., the car is 5 times smaller than the real car, meaning that its length is around 55 cm, and the car is originally equipped with a small internal combustion engine. This internal combustion engine is replaced with two electric motors each driving one rear wheel though a separate gearbox. The main components of the experimental setup are shown in Figure 2 and a functional block diagram is given in Figure 3. The electronic systems and the gearbox are designed in-house at the Eindhoven University of Technology. In the remainder of this section, all the functions indicated in Figure 3 will be described in more detail.

2.1 Remote control and front wheels steering and braking

Currently, the RC car is controlled via the standard remote controller, which sends a throttle percentage and a

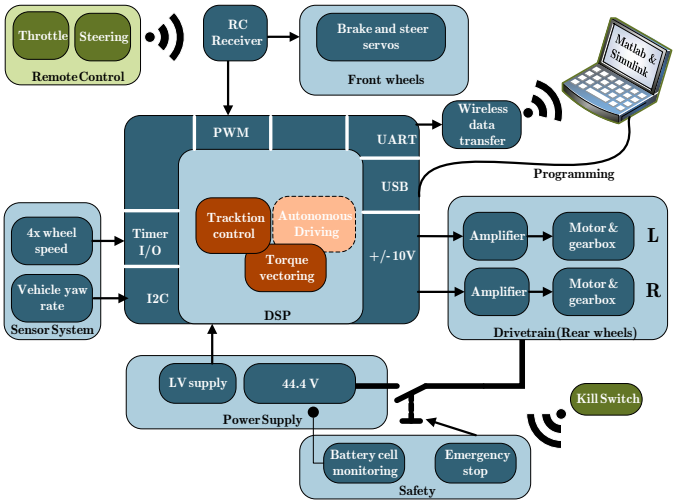

Fig. 3. Functional diagram

steering percentage to the receiver in the car. The steering percentage is directly sent to the steering servos, i.e., steering is not actively controlled via the DSP, but the signal is sent to the DSP for data logging and so that it can be used for, e.g., torque vectoring. The throttle percentage is sent to the DSP which can generate a throttle percentage for the rear left and rear right wheels. The mechanical connections to the brake servo are such that it only operates the mechanical brakes of the two front wheels. The rear wheels are braked using the electric motors.

2.2 Sensor system

The experimental setup has four wheel speed sensors and a combined gyroscope/accelerometer. The wheel speed sensors consist of black and white striping on the inside of the wheels in combination with a reflective optical sensor. Every wheel has six black and six white stripes of equal size on its circumference as shown in Figure 2. Inside the wheel, a small PCB is positioned containing the CNY70 optical sensor used to detect the black/white transitions when the wheel turns. The DSP uses the time elapsed between two transitions to calculate the speed of each individually wheel. The gyroscope/accelerometer is an MPU-6000 accelerometer, which is mounted on the back of the processor board and communicates with the DSP through an I2C communication bus.

2.3 Drive train

The drive train contains two amplifiers that will deliver power to the motors. The motors are 3-phase synchronous motors, each with a 419 W continuous power output. The amplifiers are operated as current sources, the output current is controlled using a setpoint provided by the DSP. The motor has approximately a linear relation between the current and the torque. This relation is determined by the construction of the motor and for the motors used in the car the relation is $0.044 Nm/A$. To brake the vehicle in case of an emergency, the motor windings can be short-circuited through a set of high-power resistors.

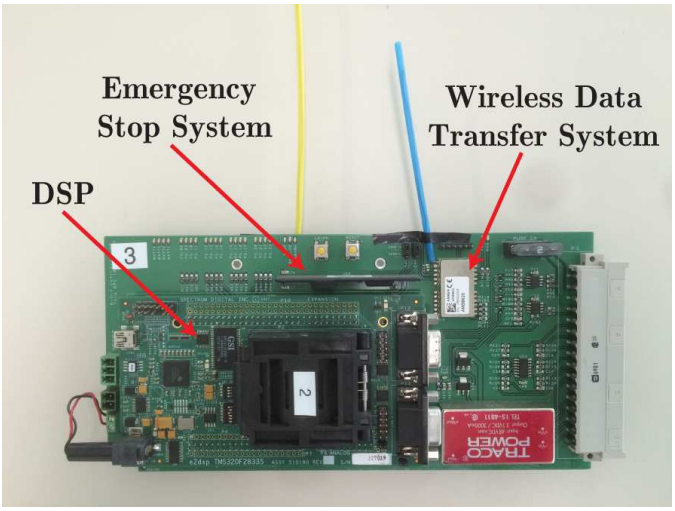

Fig. 4. Processor board with the main control unit

2.4 Power supply

The car is powered using 4 LiPo batteries connected in series resulting in an output voltage of 44.4 Volts and a total battery capacity of 4000 mAh. To provide power to the electronics, DC/DC convertors are used.

2.5 Safety

To ensure safety, a battery monitoring system keeps track of the individual voltages of each of the four batteries. If one cell voltage drops below 3 Volts, a LED will light up and a signal will be sent to the DSP. Furthermore, as soon as one of the battery cells is below 3 Volts for more than 4 seconds, the motors are de-activated. Besides a battery monitoring system, safety of the experimental setup is warranted by an Emergency Stop System that consists of a receiver that, when a kill switch button is pressed, de-activates the electric motors and short-circuits the phases of the motors to generate a braking torque.

2.6 Control unit with the DSP

Most of the control unit functions are implemented on the processor board that is shown in Figure 4. The board is equipped with the Texas Instruments (TI) eZDSP F28355 evaluation board, an AMBER Wireless Data Transfer System, the aforementioned Emergency Stop System and the gyroscope/accelerometer. The wireless data transfer system allows signals from the DSP to be send to a remote PC with a frequency of 100 Hz. The wireless data transfer system can also receive signals from the remote PC, which can be used in the future for remotely controlling the car via a remote PC. This allows the car to be used for, e.g., development of autonomous driving technology, which requires advanced distributed and networked control.

2.7 Programming and data logging software interface

Programming the DSP and logging sensor data from the RC car is done using a Matlab/Simulink-based software interface. In particular, TI eZDSP F28355 DSP is supported by Matlab's Embedded Coder, meaning that Simulink to be used to implement the controllers on the car. The AMBER Wireless Data Transfer System can be accessed as a virtual COM port, which allows measurement data to be received in real-time in Matlab. To allow for easy processing of measurement data, a graphical user interface (GUI) developed in Matlab. Having a user-friendly software interface is important as it allows students to focus on developing modeling and experimenting skills, rather than developing programming skills.

3. VEHICLE DYNAMICS MODELING

The experimental setup described in the previous section is used for teaching vehicle dynamics and control. An elementary aspect in vehicle dynamics is related to the notions of oversteer and understeer. The concept of oversteer and understeer can be analyzed with the single-track bicycle model (Pacejka, 2005) shown in Figure 5. The model will briefly be described here and it will be shown that this relatively simple model can capture the dynamics of the car well.

3.1 Bicycle model

The vehicle can be lumped into a point mass for which the equations of motion in the vehicle's longitudinal velocity u, lateral velocity v and jaw rate r can be described by the following differential equations, see e.g., (Pacejka, 2005):

$$\dot{u} = \tfrac{1}{m}F_u + vr \tag{1a}$$
$$\dot{v} = \tfrac{1}{m}F_v - ur \tag{1b}$$
$$\dot{r} = \tfrac{1}{I}M \tag{1c}$$

where F_u is the total force in u direction, F_v is the total force in v direction, M is the total moment around the center of gravity, m is the vehicles mass, and I is the moment of inertia around the jaw axis. The total forces and moments are the result forces generated through the tyres and friction forces acting on the vehicle and can be described by the following equations

$$F_u = F_{\mathrm{r}_1} + \cos(\delta)F_{\mathrm{f}_1} - \sin(\delta)F_{\mathrm{f}_2} - F_{\mathrm{d}} \tag{2a}$$
$$F_v = F_{\mathrm{r}_2} + \sin(\delta)F_{\mathrm{f}_1} + \cos(\delta)F_{\mathrm{f}_2} \tag{2b}$$
$$M = M_{\mathrm{tv}} + a(\cos(\delta)F_{\mathrm{f}_2} + \sin(\delta)F_{\mathrm{f}_1}) - bF_{\mathrm{r}_2} \tag{2c}$$

where F_{i_1} for $i \in \{\mathrm{r},\mathrm{f}\}$ are the longitudinal tyre forces with respect to the tyre orientation, F_{i_2} for $i \in \{\mathrm{r},\mathrm{f}\}$ are

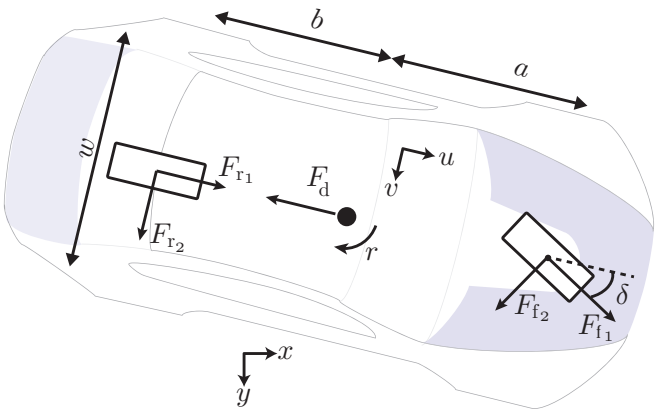

Fig. 5. Forces acting on the RC model racing car in x-y plane

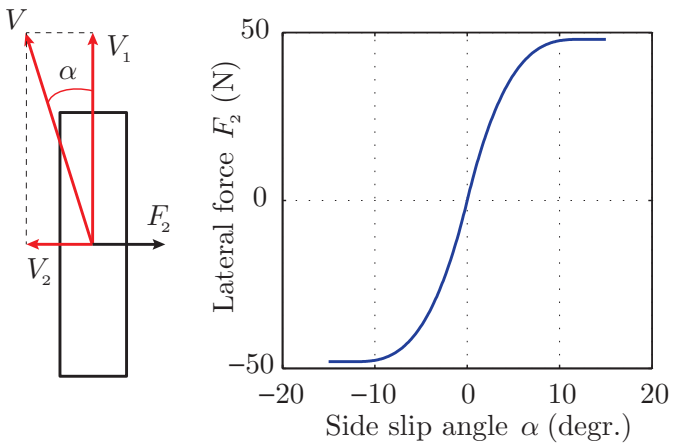

Fig. 6. Lateral forces on the wheel

the lateral tyre forces with respect to the tyre orientation, F_d is the total drag force acting on the vehicle body as a result of air drag and road slope and δ is the steering angle. The parameters a, b define the position of the center of gravity. The extra moment M_{tv} generated through torque vectoring is given by

$$M_{\mathrm{tv}} = \frac{\Delta T}{r_{\mathrm{w}}} w, \tag{3}$$

where w is the track width of the car, ΔT is the torque difference between the left and right wheel and r_{w} is the wheel radius.

3.2 Lateral and longitudinal tyre forces

The lateral tyre forces are generated through lateral tyre slip, which is defined as

$$\alpha = \arctan(\tfrac{V_2}{V_1}) \tag{4}$$

where V_2 is the lateral velocity of the tyre and V_1 is the longitudinal velocity (see Figure 6). For the rear and front tyre, the wheel slip is given by

$$\alpha_r = \arctan(\tfrac{-v+br}{u}), \tag{5a}$$
$$\alpha_f = \delta + \arctan(\tfrac{-v-ar}{u}), \tag{5b}$$

respectively. The lateral tyre forces are a nonlinear function of the side slip angle and depending on many parameters, e.g., vertical tyre force on the tyre and road surface. An example of a lateral tyre characteristic is shown in Figure 6. To reduce the complexity of the model significantly, the lateral force are approximated with a inverse tangent function given by

$$F_{\mathrm{r}_2} = C_{\mathrm{r}_1} \arctan(C_{\mathrm{r}_2}\alpha_r) \tag{6a}$$
$$F_{\mathrm{f}_2} = C_{\mathrm{f}_1} \arctan(C_{\mathrm{f}_2}\alpha_f) \tag{6b}$$

where C_{r_1}, C_{r_2}, C_{f_1} and C_{f_2} are four unknown tyre characteristics which need to be estimated.

The longitudinal tyre dynamics are not taken into account in the model such that the longitudinal forces F_{r_1} are the result of the torque from the motors and given by

$$F_{\mathrm{r}_1} = \frac{(T_{\mathrm{left}}+T_{\mathrm{right}})r_{\mathrm{gb}}}{r_{\mathrm{w}}} \tag{7}$$

where T_{right} and T_{left} are the right and left motor torque, respectively, r_{gb} is the gearbox ratio and r_{w} is the wheel radius.

3.3 Validation of bicycle model

In the presented model, the lateral tyre characteristics C_{r_i} and C_{f_i}, $i \in \{1, 2\}$, of the rear and front tyre, respectively, can be changed to adapt the properties of the car in a corner, i.e., it can be used to make the model exhibit oversteer, neutral steer or understeer. In Figure 7, the results of the vehicle model with estimated parameters is given together with measurement data. The measurement data is obtained by driving circles with a maximum steering angle and increasing velocity. The figure shows the yaw rate r as function of the longitudinal velocity u. If the car is neutral steered, the yaw rate r increases linearly with the longitudinal velocity u, which can be explained by the relation

$$u = \frac{a+b}{\tan(\delta)} r \tag{8}$$

where $\frac{a+b}{\tan(\delta)}$ is the radius of the driven circle which is constant for a neutral steered vehicle. For an understeered vehicle, the yaw rate decreases as function of longitudinal velocity as the driven radius becomes larger. Figure 7 clearly shows that the RC model racing car exhibits understeer and that we can approximated the lateral vehicle dynamics well using the bicycle model with relatively simple tyre characteristics.

4. CONTROLLER DESIGN

With the electronic differential, a different torque can be send to each of the rear wheels which results in an extra moment given by (3). As a result, the moment on the vehicle given by (2c) can be increased or decreased, thereby changing the yaw rate of the vehicle. Moreover, the traction force on each of the rear wheels can be controlled such that excessive wheel slip does not occur and the vehicle remains stable. Examples of a control solution for these two problem are presented in this section. There exist many more and better control solutions, but those are beyond the scope of a second-year Bachelor's course.

4.1 Yaw rate control

By controlling the yaw rate of the RC car, the understeered car can be compensated to a neutral steered or oversteered vehicle. Most students taking our course design the yaw rate controller such that the car becomes neutral steered, which is assumed to give a better steering response to the driver (Rieveley and Minaker, 2007). The preferred behavior is dependent on the application, however, e.g., for a rally racing car, an oversteered vehicle is desired when

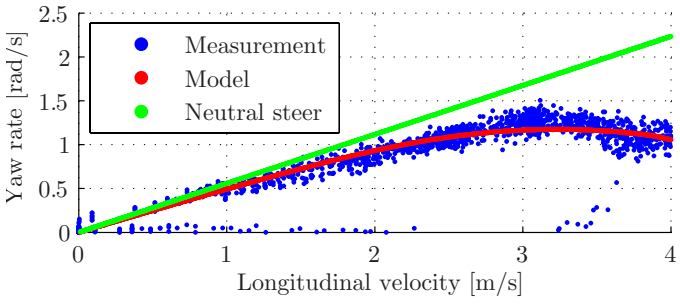

Fig. 7. Bicycle model compared with measurement data

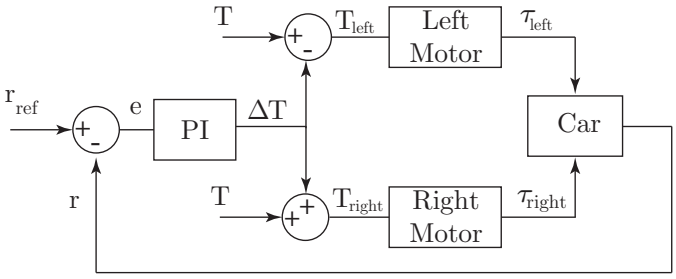

Fig. 8. Yaw rate control

cornering through a sharp corner, i.e., the driven radius should be small.

In neutral steer, the yaw rate is given by

$$r_{\text{ref}} = \frac{\tan(\delta)}{a+b} u. \tag{9}$$

which is derived from (8) and is used as a reference signal for the controller. To track this reference signal, a PI controller is designed. A schematic of the controller is shown in Figure 8. The PI controller regulates the throttle difference between the left and right motor as function of the error between the reference yaw rate and the actual yaw rate, i.e.,

$$\Delta T = (K_{\text{p}} + \frac{K_{\text{i}}}{s})(r_{\text{ref}} - r), \tag{10}$$

where K_p is the proportional gain and K_i is the integral gain. The throttle difference is then added to the right motor and subtracted from the left motor, i.e.,

$$T_{\text{right}} = T + \Delta T, \tag{11}$$
$$T_{\text{left}} = T - \Delta T, \tag{12}$$

which result in a torque T_{right} at the right wheel and a torque T_{left} at the left wheel.

4.2 Traction control

Too much torque can lead to excessive wheel slip on the rear wheels which lowers the maximal tire force in both longitudinal and lateral direction which eventually leads to excessive oversteer, i.e., instability of the RC car. To avoid this situation, a traction controller needs to be designed. We will show the design for the left rear wheel only, as the design for the right rear wheel is exactly the same. If we assume that the wheel slip on the front wheels is small, which is a reasonable assumption for a rear wheel driven car, then we can approximate the wheel slip of the left rear wheel by

$$\kappa_{\text{left}} = \frac{\omega_{\text{r,left}} - \omega_{\text{f,left}}}{\omega_{\text{f,left}}}, \tag{13}$$

which is not well defined for low speeds, i.e., when $\omega_{\text{f,left}} \approx 0$. Instead, we limit the wheel slip by upper bounding the left rear wheel speed as function of the left front wheel speed, i.e.,

$$\omega_{\text{r,left}} \leqslant \gamma \omega_{\text{f,left}} \tag{14}$$

where $\gamma > 1$ determines the maximum allowable wheel slip which depends on the road surface and tyre characteristics. In this example, we use a PI controller that starts regulating the torque of the motor if the rear wheel speed exceeds the maximum speed given by (14). For the left rear wheel, this is given by

$$T_{\text{left}} = (K_{\text{p}} + \frac{K_{\text{i}}}{s})(\omega_{\text{ref,left}} - \omega_{\text{r,left}}), \tag{15}$$

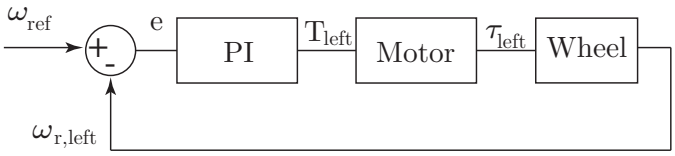

Fig. 9. Traction control

where $\omega_{\text{ref,left}} = \gamma \omega_{\text{f,left}}$ is the reference value, K_p is the proportional gain and K_i is the integral gain. The control scheme is shown in Figure 9. If the rear wheel speed satisfies (14), the PI controller is deactivated.

5. DEMONSTRATION

In this section we will show some results of the control solutions presented in the previous section.

5.1 Yaw rate control

The yaw rate controller is implemented on the DSP. To measure the performance of the controller, the car is driven in circles with a constant steering angle and increasing velocity. The results are shown in Figure 10. The blue dots are without the yaw rate controller, the red dots are with yaw rate controller. The figure nicely shows that the yaw rate controller does make the car more neutral steered. At higher velocities, however, i.e., speeds over 3 m/s, the tyre limitations start kicking in and neutral steer cannot be achieved anymore. The results obtained here are not optimal in performance but give a flavor of what students can achieve during the course.

5.2 Wheel slip control

The wheel slip controller is implemented on the DSP and tested with a straight line acceleration test with a step of 70 % throttle. The results without a wheel slip controller are shown in Figure 11. It clearly shows that the rear wheels show excessive wheel slip. Moreover, at $t = 4.2$ s, the RC car has become unstable as the front right wheel has a larger velocity than the front left wheel which means that the vehicle is turning to the left (even though the vehicle is not steered using the steering wheel).

The results with the wheel slip controller are shown in Figure 12. The result show that the excessive wheel slip of the rear wheels is reduced. The rear left wheels shows

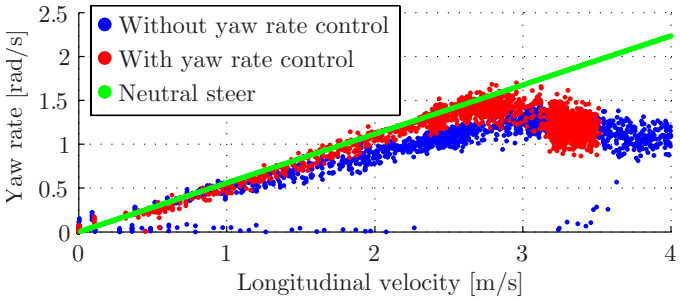

Fig. 10. Yaw rate as function of longitudinal velocity with and without yaw rate controller

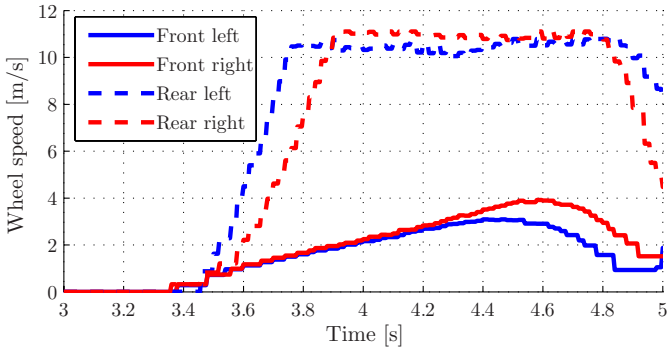

Fig. 11. Straight line acceleration without traction control

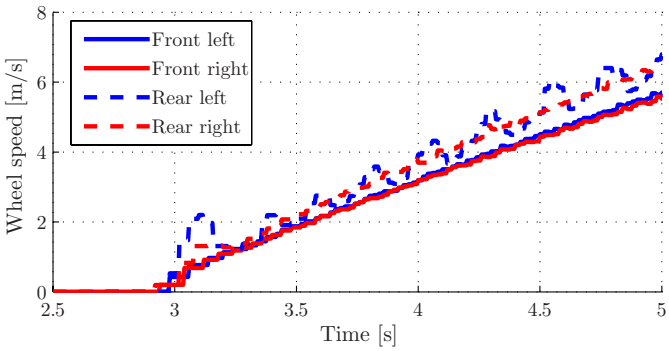

Fig. 12. Straight line acceleration with traction control

more oscillations around the setpoint than the rear right wheel indicating that the right wheel has mechanically more damping due to friction. Nevertheless, the controller performs well as can be seen by the straight acceleration of the car observed by the front wheel speeds.

6. DISCUSSION AND CONCLUSIONS

In this paper, we have presented a custom-made radio-controlled (RC) model racing car and a modeling and control challenge that can be tackled using this car. The RC car is used to give second-year Bachelor students hands-on experience which is essential for a well balanced education. We modeled the RC car using a bicycle model showing that this simple model can capture the essential vehicle dynamics. Furthermore, we presented and experimentally demonstrated control solutions for torque vectoring and traction control. Because of the wireless communication link between the RC racing car and a remote PC, it is also an excellent platform for developing automotive driving technology, which requires advanced distributed and networked control.

ACKNOWLEDGEMENTS

The authors would like to thank the teaching assistants Mannes Dreef, Julien Duclos, Feye Hoekstra, Zuan Khalik, Maarten van Rossum and Bas Scheepens for their assistance in teaching the course and the over 100 BSc students taking the course for their enthusiasm.

REFERENCES

Bianchi, D., Borri, A., Di Benedetto, M.D., Di Gennaro, S., and Burgio, G. (2010). Adaptive integrated vehicle control using active front steering and rear torque vectoring. *International Journal of Vehicle Autonomous Systems*, 8(2-4), 85–105.

De Novellis, L., Sorniotti, A., Gruber, P., and Pennycott, A. (2014). Comparison of feedback control techniques for torque-vectoring control of fully electric vehicles. *IEEE Transactions on Vehicular Technology*, 63(8), 3612–3623.

Kaiser, G., Holzmann, F., Chretien, B., Korte, M., and Werner, H. (2011). Torque vectoring with a feedback and feed forward controller-applied to a through the road hybrid electric vehicle. In *Intelligent Vehicles Symposium (IV), 2011 IEEE*, 448–453. IEEE.

Pacejka, H. (2005). *Tire and vehicle dynamics*. Elsevier.

Piyabongkarn, D., Lew, J.Y., Rajamani, R., Grogg, J.A., and Yuan, Q. (2007). On the use of torque-biasing systems for electronic stability control: limitations and possibilities. *IEEE Transactions on Control Systems Technology*, 15(3), 581–589.

Rajamani, R. (2006). Electronic stability control. *Vehicle Dynamics and Control*, 221–256.

Rieveley, R.J. and Minaker, B.P. (2007). Variable torque distribution yaw moment control for hybrid powertrains. Technical report, SAE Technical Paper.